

vLPD-Net: A Registration-aided Domain Adaptation Network for 3D Point Cloud Based Place Recognition

Zhijian Qiao^{1†}, Hanjiang Hu^{1†}, Siyuan Chen¹, Zhe Liu², Zhuowen Shen¹, Hesheng Wang^{1*}

¹Shanghai Jiao Tong University, ²University of Cambridge

Abstract

In the field of large-scale SLAM for autonomous driving and mobile robotics, 3D point cloud based place recognition has aroused significant research interest due to its robustness to changing environments with drastic daytime and weather variance. However, it is time-consuming and effort-costly to obtain high-quality point cloud data and groundtruth for registration and place recognition model training in the real world. To this end, a novel registration-aided 3D domain adaptation network for point cloud based place recognition is proposed. A structure-aware registration network is introduced to help learn feature from geometric properties and a matching rate based triplet loss is involved for metric learning. The model is trained through a new virtual LiDAR dataset through GTA-V with diverse weather and daytime conditions and domain adaptation is implemented to the real-world domain by aligning the local and global features. Extensive experiments have been conducted to validate the effectiveness of the structure-aware registration network and domain adaptation. Our results outperform state-of-the-art 3D place recognition baselines on the real-world Oxford RobotCar dataset with the visualization of large-scale registration on the virtual dataset.

1. Introduction

In the applications of autonomous driving and mobile robotics, place recognition plays an essential role in the perception and localization. Based on a well-built database of point cloud or images, place recognition aims to retrieve the most similar frames given the query LiDAR scan or camera input. However, since it is of great necessity for the outdoor autonomous vehicle to work from a long-term perspective, the changes of illumination, weather and daytime cast a huge challenge for the place recognition and retrieval tasks. It has been shown that the point cloud based algorithm is more robust to the changing environmental conditions [3, 18].

[†]Equal Contribution, *Corresponding Author

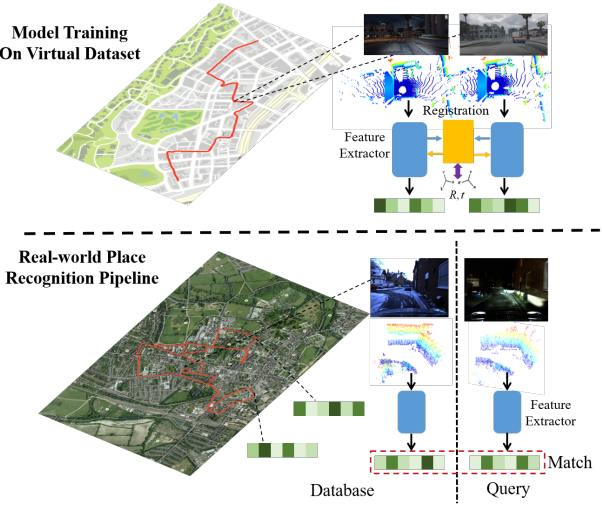


Figure 1. The model training and place recognition pipeline is shown above. The model is trained on the virtual dataset for structure-aware feature representation through point cloud registration. For testing, the point cloud with the most similar feature is retrieved given query point cloud feature under changing environments.

In order to further improve performance and generalization ability for point cloud based place recognition, it is indispensable to obtain a large amount of high-quality training data. Nevertheless, it is effort-costly and time-consuming to collect real-world datasets across different types of environments [21]. Consequently, the synthetic virtual dataset [45] has been utilized through GTA-V to involve multi-environment traverses without laborious effort, while there is a severe gap between synthetic domain and real-world domain for place recognition [13]. Besides the domain adaptation of global features, the local features of point cloud vary a lot across domains and feature alignment is also implemented in [25].

However, the previous NetVLAD based work on point cloud based place recognition [3, 18] mainly focuses on the global feature representation, missing the structure information of point cloud, *e.g.*, it only learns how many trees exist, ignoring the relative pose of them. For the consideration

that the point-wise feature can be extracted with the spatial coordinates and geometric information in the point cloud registration [6, 43], we incorporate the point cloud registration to guide feature extraction layer and then propose a matching rate based triplet loss from registration network for metric learning.

In this work, we propose a novel registration-aided 3D domain adaptation model through an effective large-scale point cloud description network trained on the virtual dataset (vLPD-Net) for point cloud based place recognition. A structure-aware registration network with the light-weighted conditional attention mechanism is proposed to leverage geometry property and co-contextual information between two input point clouds. Furthermore, a matching rate based triplet loss generated by an iterative scheme is involved in metric learning. Along with them, the adversarial training pipeline is implemented to align the local and global features. In the experiment, due to effective domain adaptation from synthetic to real-world datasets for representation learning, our method outperforms state-of-the-art point cloud based place recognition baselines on the Oxford RobotCar dataset. To the best of our knowledge, we are the first to address the outdoor large-scale point cloud based place recognition through domain adaptation with the assistance of point cloud registration. The model training and place recognition pipeline is illustrated in Figure 1.

Our contribution could be summarized as follows:

- A novel registration-aided domain adaptation model, vLPD-Net, is proposed for the robust large-scale outdoor point cloud based place recognition with feature alignment from synthetic to the real-world domain.
- A structure-aware registration network is introduced with a light-weighted conditional attention mechanism to learn the co-contextual information, an efficient outlier removal algorithm, and a new matching rate based triplet loss for metric learning.
- A multi-environment virtual point cloud training set is built and the effectiveness of the proposed model is validated through the state-of-the-art performance on the real-world Oxford RobotCar dataset for place recognition and on the large-scale virtual dataset for registration with visualization.

2. Related Work

2.1. Point Cloud Based Place Recognition

As 3D LiDAR has been widely used in outdoor autonomous driving and mobile robotics, the point cloud is becoming increasingly important for perception and localization. As for the 3D data analysis, traditional feature descriptors [8, 14, 27, 28, 30] are hand-crafted and not robust

to noise, uniform density and sparsity. Deep learning based methods [15, 17, 23, 24, 40, 49] successfully learn the effective point cloud feature and perform impressive results on multiple tasks. For the point cloud based place recognition task, PointNetVLAD [3] is the first end-to-end model to extract global feature of point cloud by combining PointNet and NetVLAD. PCAN [48] incorporates attention mechanism into PointNetVLAD to learn representation with salient regions. Recent work LPD-Net [18] takes local structural and spatial distribution information into account which achieves state-of-the-art place recognition performance. PIC-Net [20] fuses the point cloud and image information through the attention mechanism for robust representation. OREOS [31] proposes a retrieval-based localization method from the well-built dense point cloud map for the query point cloud frame.

2.2. Point Cloud Registration

Point cloud registration aims to find the rigid transformation from source to target point cloud frames. Traditional ICP-based methods optimize the matching points and the pose transformation with the consideration of the sparsity and noise of point cloud. However, they tend to reach local optimization and are sensitive to the initial pose estimation. Other methods like RANSAC [27], GO-ICP [42], FGR [50] try to find the global optimization but suffer from the time cost due to the large ratio of outliers while recent TEASER++ [41] is more robust to the outliers with robust and effective feature input. Deep neural networks provide more distinguishable features recently. RPM-Net [44] proposes Sinkhorn [34] layer to predict a doubly stochastic matrix to represent the matching relationship of point cloud. 3Dfeatnet [43] proposes the cluster matching based metric learning while recent D3feat-NET [4] detects local features and learns the feature matching simultaneously. DGR [6] proposes three modules to solve pose from a set of putative correspondences accurately and robustly. To fully use the correlation of the matching points, the transformer is introduced to find the soft matching points in DCP [38] and PRNet [39]. However, it is difficult and memory-costly to train the attention layers effectively due to a large amount of outdoor point cloud, leading to the even distribution of attention weight for each point.

2.3. Unsupervised Domain Adaptation

Unsupervised domain adaptation (UDA) aims to address the gap of the distribution between training set and the test set. Feature alignment [7, 10, 22, 35, 37, 47] is implemented to bridge the gap through cross-domain shared latent feature space. CORAL [36], Geodesic distance [11] and Maximum Mean Discrepancy (MMD) [5, 19] try to increase the difference between the classes while decreasing the difference inside the classes. Domain-invariant features [12, 16, 32]

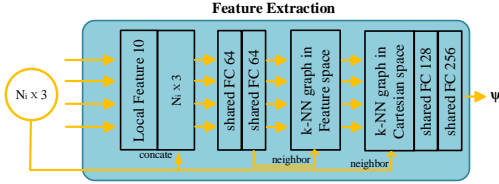


Figure 2. LPD network architecture for feature extraction.

are also used for representation learning through neural networks to achieve domain adaptation. Besides, adversarial training is widely used through discriminator distinguishing the generated features from two domains, like Domain Adversarial Network (DAN) [9] and Maximum Classifier Discrepancy (MCD) [29]. Recent work for 3D point cloud data domain adaptation, PointDAN [25], proposes a general framework to align both local and global features from source to target domains through adversarial training. However, PointDAN only focuses on object point cloud and it does not apply to the large-scale outdoor scene, where the key points are distributed scarcely and unevenly.

3. vLPD-Net Model

3.1. Problem Formulation and System Overview

For the problem of point cloud place recognition, the final retrieval is determined through the selection with the most similarity in the database given the query point cloud frame. Denote the samples in the database as

$$\mathbb{P}_{DB} = \{P_i \in \mathbb{R}^{N \times 3} | i = 1, 2, \dots, M\} \quad (1)$$

$$P_i = \{p_j \in \mathbb{R}^3 | j = 1, 2, \dots, m_i\}$$

where there are M frames of point cloud in the database and m_i points in each point cloud frame. The problem in this work could be formulated to train the place recognition model on the virtual dataset \mathbb{P}_V , representing the robust feature f_V for the point cloud frame P_V . In testing, the retrieval on the real-world dataset \mathbb{P}_R is implemented through the similarity in the database given the query the feature representation f_R . To be concise and informative, the virtual point cloud is denoted as P while the real-world on is P_R .

The registration-aided domain adaptation architecture, vLPD-Net, is shown in Figure 3, which contains the parts of feature extraction layer, structure-aware registration network(S-ARN), metric learning module and the adversarial training pipeline. Given an example of two input point clouds P and Q ,

$$P = \{p_i \in \mathbb{R}^3 | i = 1, \dots, N\} \quad (2)$$

$$Q = \{q_i \in \mathbb{R}^3 | i = 1, \dots, N_q\} \quad (3)$$

a feature extraction layer, a structure-aware registration network and a locally aggregated network are sequentially

used to encode P and Q into two global descriptor $f_P = h(g(\mu(P), \mu(Q)))$ and $f_Q = h(g(\mu(Q), \mu(P)))$ respectively. Function μ extracts point-wise feature ψ , function g downsamples ψ to a fixed quantity K , and function h represents clusters the local features into a global descriptor f .

3.2. Feature Extraction

Recently, there are many feature extraction layers that are compatible with the place recognition pipeline. We adopt LPD-Net [18] (shown in Figure 2) as μ due to its excellent performance on the large-scale place recognition. Adaptive local feature extraction is introduced to address the sparsity and uniform density of point. It is validated to improve the performance using graph-based feature aggregation in the Cartesian space as the last feature aggregation operation. Through this layer, ψ_P and ψ_Q can be obtained by $\mu(P)$ and $\mu(Q)$ respectively.

3.3. Structure-Aware Registration Network

After well-aggregated neighboring information is learned in the high-dimension space, the point-wise feature goes through a structure-aware registration Network to benefit from the spatial and geometric information. The co-contextual information of 3D point cloud pairs is explored for the latent embedding. Inspired from the widely-used Transformer module in natural language processing, the contextual information is encoded through self & conditional attention mechanism for the input embedding in [38, 39]. However, because of the laborious calculation for element-wise correlation distribution, the original transformer module cost $O(N^2)$ time and memory given the element quantity of N .

Based on the observation that the attention distribution from the points of one point cloud to the other tends to be uniform in Transformer under the outdoor large-scale scenes with a large number of points, we design a novel light-weighted attention mechanism. Each point of one point cloud shares the attention weight to the other so that the complexity is $O(N)$ for N points and a function that maps $\mathbb{R}^{N_x \times C} \times \mathbb{R}^{N_y \times C}$ to $\mathbb{R}^{N_x \times C}$, where C is feature dimension of ψ and $N_x \neq N_y$, is described as

$$z_P = \psi_P + \theta(\psi_P, \psi_Q) \quad (4)$$

$$z_Q = \psi_Q + \theta(\psi_Q, \psi_P) \quad (5)$$

And θ is defined as

$$\theta(\psi_x, \psi_y) = W_3 \psi_y \odot \delta(W_1 \mathbb{E}(\psi_x) \odot W_2 \mathbb{E}(\psi_y)) \quad (6)$$

where $\mathbb{E}(\psi_x)$ and $\mathbb{E}(\psi_y)$ indicates the mean of point-wise feature in the spatial channel, $W_{1,2,3}$ represents convolutional layer with 1×1 kernel, \odot represents dot product

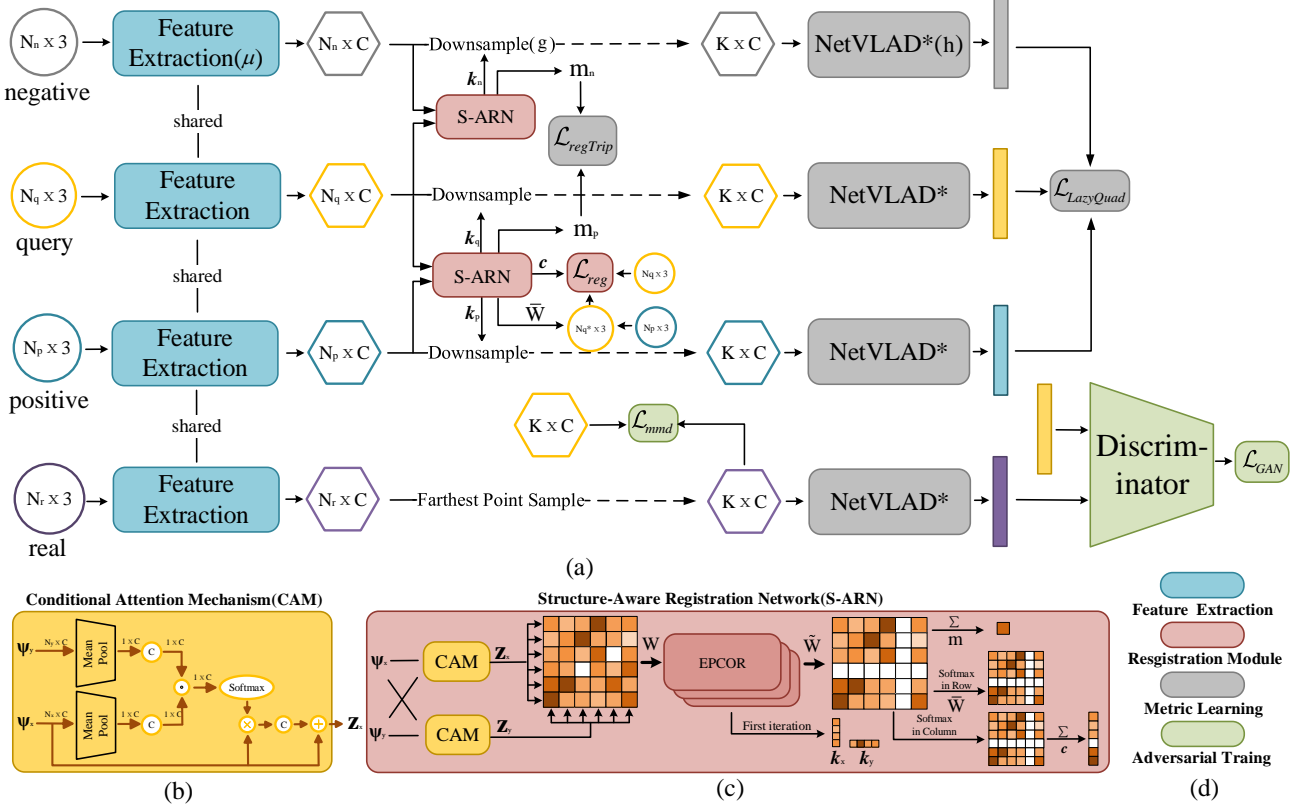


Figure 3. (a) Overview of vLPD-Net. (b) Detail conditional attention mechanism (CAM) network. (c) Structure-aware registration network (S-ARN). (d) Colors of different parts about their networks and losses.

with automatic expansion of dimensions and δ function represents Sigmoid function respectively.

Given z_P and z_Q of two point clouds, we define a distance in the feature space to generate the matching matrix $W \in \mathbb{R}^{N \times N_q}$. In this work, ℓ^2 distance is used to define every element of W as

$$W(i, j) = \|z_P^i - z_Q^j\|_2, i = 1 \dots N, j = 1 \dots N_q \quad (7)$$

After that, a simple but efficient iteration scheme, named Efficient Point Cloud Outlier Removal (EPCOR), is proposed to remove the non-matching point cloud outliers to obtain sparse matching matrix \tilde{W} and confidence vector c for pairwise registration. The complete algorithm is described in Algorithm 1.

For every point p_i in P , its soft matching point p_i^* is generated with the sparse weighted sum of points in Q through the equation below:

$$p_i^* = \frac{1}{\sum_{j=1}^{N_q} \tilde{W}(i, j)} \sum_{j=1}^{N_q} \tilde{W}(i, j) q_j \quad (8)$$

Each matching pair (p_i, p_i^*) is weighed by the sparse confidence vector c for removing outlier non-matching pair,

and R and t can be solved by a weighted procrustes method in [6, 44]. The loss of registration network is denoted as the ℓ^2 distance between the generated matching points p_i^* and p transformed using the groundtruth transformation \hat{R} and \hat{t} :

$$\mathcal{L}_{reg} = \frac{1}{\sum_{i=1}^N c_i} \sum_{i=1}^N c_i \|p_i^* - (\hat{R}p_i + \hat{t})\|_2 \quad (9)$$

In this section, the input K of Algorithm 1 represents the downsampling number, and the intermediate variable k and k_q is used in the function g as the downsampling index to downsample ψ_P and ψ_Q to $\bar{\psi}_P$ and $\bar{\psi}_Q$, which share a fixed size K .

3.4. Metric Learning

In each iteration process, the anchor point cloud P_a together with positively paired point cloud P^+ and negatively paired point cloud P^- is sampled by function g . To represent the point cloud for effective place recognition, we adopt the metric learning strategy [3] to use a lazy quadruplet strategy, which involves the hardest negative pairs in the original triplet loss and also a NetVLAD layer followed by a fully connected layer is denoted as NetVLAD*, which represents function h in Section 3.1. Denote the triplet input as

Algorithm 1 Efficient Point Cloud Outlier Removal (EPCOR)

Input: $W \in \mathbb{R}^{N \times N_q}$, $K \in \mathbb{R}^1$
Output: $\tilde{W} \in \mathbb{R}^{N \times N_q}$, $c \in \mathbb{R}^{N \times 1}$, $k, k_q \in \mathbb{R}^{K \times 1}$, $m \in \mathbb{R}^1$

$$[w_1^T, w_2^T, \dots, w_N^T]^T = W, w_i \in \mathbb{R}^{1 \times N_q}$$

$$[m_1, m_2, \dots, m_{N_q}] = W, m_i \in \mathbb{R}^{N \times 1}$$

$$s_0 = 0, \delta_s = 1, \bar{W} = W, iter = 0$$

while $\delta_s > 0.05$ **do**

$iter = iter + 1$

for i in $range(N)$ **do**

$w_i' = softmax(w_i)$

$m_i' = softmax(m_i)$

end for

$r = \sum_{i=1}^N w_i', \quad c = \sum_{i=1}^{N_q} m_i'$

if $iter == 1$ **then**

choose index of $TopK(c)$ as k and index of $TopK(r)$ as k_q

end if

$I_r = \bigcup_i (r(i) < \tau), \quad I_c = \bigcup_i (c(i) < \tau)$

$s = \frac{|I_r| + |I_c|}{N + N_q}$

$\delta_s = s_{iter} - s_{iter-1}$

$W(I_r, :) = 0, \quad W(:, I_c) = 0$

end while

$\tilde{W} = W$

$c = \frac{c}{\|c\|_1}$

$m = \sum_{i,j=1}^{N, N_q} W / \bar{W}$

return \tilde{W}, c, k, k_q, m

$\mathcal{T} = (P_a, P^+, \{P^-\})$. P^{-*} is sampled to be dissimilar to all others in \mathcal{T} to avoid the reduction of distance among dissimilar point clouds in negative samples. The lazy quadruplet loss could be formulated as below:

$$\delta^+ = \|f(P_a) - f(P^+)\|_2 \quad (10)$$

$$\forall P_j^- \in \{P^-\}, \delta_j^- = \|f(P_a) - f(P_j^-)\|_2 \quad (11)$$

$$\forall P_k^- \in \{P^-\}, \delta_k^{-*} = \|f(P^{-*}) - f(P_k^-)\|_2 \quad (12)$$

$$\begin{aligned} \mathcal{L}_{lazyQuad} = & \max_j ([\alpha + \delta^+ - \delta_j^-]_+) \\ & + \max_k ([\beta + \delta^+ - \delta_k^{-*}]_+) \end{aligned} \quad (13)$$

Moreover, considering a simple assumption that dissimilar scenes share fewer inliers in the registration network, we use return value m from Algorithm 1, which indicates what percentage of inliers remains. To this end, we propose an matching rate based distance function σ , e.g., for positive pair, $\sigma^+ = m^+$ and for negative pair, $\sigma^- = m^-$. A

novel matching rate based triplet loss for metric learning is as follows:

$$\mathcal{L}_{regTrip} = \max(\sigma^- - \sigma^+ + \gamma, 0) \quad (14)$$

where γ is a another constant parameter giving the margin.

3.5. Adversarial Training Pipeline

Denote virtual point cloud as $P_V \sim p_V(P)$ and real-world point cloud as $P_R \sim p_R(P)$, and point-wise feature from function μ as ψ_{P_V} and ψ_{P_R} accordingly. While NetVLAD* clusters the local features into a compact global descriptor vector, the geometric local information will be missing. To this end, function g downsamples ψ_{P_V} and ψ_{P_R} to $\bar{\psi}_{P_V}$ and $\bar{\psi}_{P_R}$ where for ψ_{P_V} , g is defined in section 3.3 and for ψ_{P_V} , g refers to Farthest point sampling (FPS). Consequently, the MMD loss [5, 19] is adopted as below:

$$\begin{aligned} \mathcal{L}_{MMD} = & \mathbb{E}_{P_V \sim p_V(P), P_R \sim p_R(P)} \left[\frac{1}{n_r n_r} \sum_{i,j=1}^{n_r} \kappa(\bar{\psi}_{P_R}^i, \right. \\ & \left. \bar{\psi}_{P_R}^j) + \frac{1}{n_r n_v} \sum_{i,j=1}^{n_r, n_v} \kappa(\bar{\psi}_{P_R}^i, \bar{\psi}_{P_V}^j) \right. \\ & \left. + \frac{1}{n_v n_v} \sum_{i,j=1}^{n_v} \kappa(\bar{\psi}_{P_V}^i, \bar{\psi}_{P_V}^j) \right] \end{aligned} \quad (15)$$

For the representation feature from the NetVLAD* layer, adversarial training is adopted to make the distribution from virtual domain consistent with that from real-world domain. The discriminator is introduced to distinguish the representation from the virtual domain from that from the real-world domain. The generation and discrimination GAN losses are shown as below.

$$\begin{aligned} \mathcal{L}_{Dis} = & \mathbb{E}_{P_V \sim p_V(P), P_R \sim p_R(P)} [0.5 \times (D(f(P_R) - 1)^2 \\ & + D(f(P_V))^2)] \end{aligned} \quad (16)$$

$$\mathcal{L}_{Gen} = \mathbb{E}_{P_V \sim p_V(P)} [0.5 \times D(f(P_V) - 1)^2] \quad (17)$$

For the adversarial training, a discriminator D is proposed through a four-layer fully connected network. The optimization of discrimination is instructed by the following loss.

$$\min_D \mathcal{L}_{Dis} \quad (18)$$

While the optimization of generation is for the feature extractor, structure-aware registration network and NetVLAD* module, denoted as G to include all three networks. The involved losses are registration loss (9), triplet loss (14), lazy quadruplet loss (13), MMD loss (15) and GAN loss (17), which are shown below.

Table 1. Environment Description of the Training Set

Environment Name	Rain	Snow	Dusk	Night	Overcast	Sunny	Cloudy
Weather	Rain	Snow	Clear	Clear	Overcast	Sunny	Cloudy
Time	10:00 AM	10:00 AM	5:00 PM	11:00 PM	10:00 AM	10:00 AM	8:00 AM
Number of Point Cloud Frames	1665	1766	1464	1333	1402	1270	1260

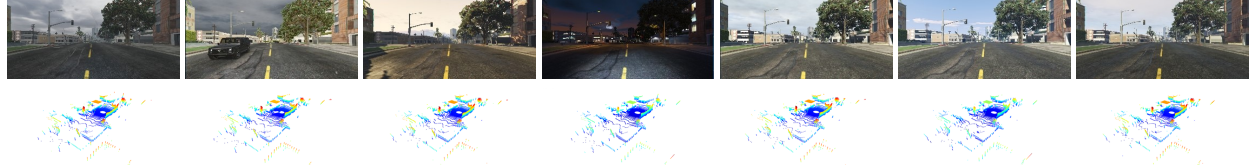


Figure 4. The RGB and the point cloud samples in the dataset. The environments for each column are Rain, Snow, Dusk, Night, Overcast, Sunny and Cloudy respectively.

4.1. Experimental Setup

$$\begin{aligned}
 & \min_G \mathbb{E}_{P_V \sim p_V(P), P_R \sim p_R(P)} [\lambda_{lazyQuad} \mathcal{L}_{lazyQuad}] \\
 & + \mathbb{E}_{P_V \sim p_V(P)} [\lambda_{reg} \mathcal{L}_{reg} + \lambda_{regTrip} \mathcal{L}_{regTrip}] \quad (19) \\
 & + \lambda_{MMD} \mathcal{L}_{MMD} + \mathcal{L}_{Gen}
 \end{aligned}$$

where λ for each term is the weight for the multi-task train-

Table 2. Experiment Comparison Results on RobotCar Dataset

	Recall@1%	Recall@1
PN-VLAD baseline [3]	81.01	62.76
PN-VLAD refined [3]	80.71	63.33
PCAN [48]	86.40	70.72
LPD-Net R [18]	94.92	86.28
LPD-Net V+R [18]	89.96	81.16
LPD-Net V	34.56	32.18
vLPD-Net V (ours)	72.9	58.8
vLPD-Net V+R (ours)	96.58	90.14

ing in the generation optimization. Note that only the virtual point cloud data are involved in the registration-related losses (9, 14).

4. Experiment

In this section, we first build a virtual point cloud dataset and specify the experimental setting for preparation. In the experiment, the model is mainly trained on the synthetic virtual dataset using high-quality data and groundtruth, while the real-world dataset is used for the alignment of representation distribution. The comparison experimental results validate the effectiveness of the proposed model. Besides, the virtual large-scale registration results are also compared to other baselines with the promising results.

To train the model using low-cost and high-quality point cloud traverses under multiple environments, followed by the previous work [26, 46], we build the virtual synthetic dataset through Grand Theft Auto V (GTA-V) with plugins [1, 2]. The point cloud together with the GPS data has been collected by controlling the movement of the car under the game environments with 7 changing weather and the daytime in Table 1 along the same route about 2.5km. The average distance between neighboring frames is 2m under every single environment. The pitch range of the Virtual lidar is -25° 15° (taking horizontal as 0°), while the horizontal range is 360° , and the maximum laser detection distance is 120m. The collected RGB and point cloud samples are shown in Figure 4. For the loss of point cloud registration, we adopt the ICP algorithm on the basis of GPS as the initial pose to obtain the high-quality rigid transformation as groundtruth. To train the the model effectively for representation learning, the distance between each frame is set to be 20m, resulting 1,016 virtual point cloud frames under 7 environments.

During the process of adversarial training, the real-world dataset Oxford RobotCar [21] is used to align the feature representation. The traverses in the Oxford RobotCar dataset are under multiple environments which is consistent with those in Table 1. The Oxford RobotCar dataset is collected using the SICK LMS-151 2D LiDAR scan together with the GPS along a route of 10km in Oxford, UK. The 3D point cloud submap is aggregated from the 2D vertical scanning LiDAR every 20m-long trajectory. Following the setting of PointNetVLAD [3] and LPD-Net [18], 21,711 training submaps from the 44 sets of data are used to train the model together with the synthetic data. For the performance evaluation, we use 3030 testing submaps.

To input the data for model training, the virtual point

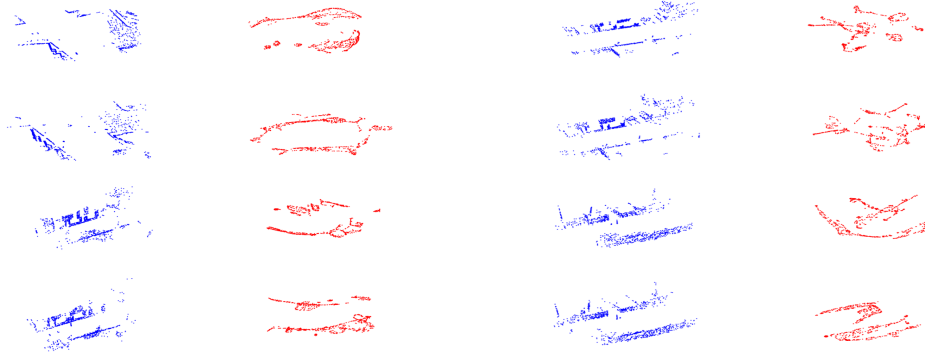


Figure 5. The samples of the original point cloud(blue) and the t-SNE visualized feature(red). The left column shows the results of vLPD-Net with registration network while the right column is not with registration network.

Table 3. Place Recognition Ablation Study on Oxford RobotCar Dataset

Registration Loss	Matching Rate Triplet Loss	MMD Loss	Adversarial Training	Avg Recall@1%	Avg Recall@1
✗	✓	✓	✓	95.88	89.40
✓	✗	✓	✓	93.79	87.56
✓	✓	✗	✓	95.67	89.27
✓	✓	✓	✗	91.44	86.58
✓	✓	✓	✓	96.58	90.14

cloud is truncated within 80 meters and normalized to [-1,1]. The voxel grid filter and random filter are used to down-sample to 4096 points, following the ground and outlier removal. While the real-world submap is sampled inside a rectangle with a length of 25 meters and a width of 10 meters, normalizing to the range of [-1,1] with the ground removed and down-sampling to 4096 points. For the EPCOR Algorithm 1, the τ is set to be 0.5 and the input K is 4096 in the experiment. For the metric learning, the margins in Equation (13, 14) are specified as $\alpha = 0.5$, $\beta = 0.2$, $\gamma = 0.5$. The weight hyperparameters in Equation (19) are given as $\lambda_{lazyQuad} = 1$, $\lambda_{reg} = 0.1$, $\lambda_{regTrip} = 0.1$ and $\lambda_{MMD} = 1$. For the point cloud registration, We directly use the registration network in the vLPD-Net to regress the 6DoF pose given the two virtual point cloud frames. The test set is split from the untrained collected synthetic dataset, with about 224 pairs of point cloud frames together with the groundtruths of 6-DoF pose. All experiments are conducted on two 2080Ti GPU.

4.2. Place Recognition Results

For the cross-environment point cloud place recognition, the same scene as the query frame is supposed to be retrieved in the database. The target descriptor vector in the database is closest to the query descriptor vector in the Euclidean distance. To evaluate the performance of large-scale place recognition, we use Average Recall@1% and Average Recall@1. The state-of-the-art baselines we choose

are the PointNetVLAD [3], PCAN [48] and LPD-Net [18]. Moreover, for the fair comparison, we compare the results of LPD-Net and our vLPD-Net using different training datasets, *i.e.* V for virtual dataset and R for real-world dataset. Note that the single V of ours indicates that the metric learning in Equation (13) is conducted on the virtual dataset, and the real-world frames are only involved in the domain adaptation in Equation (19).

From the experimental results of place recognition in Table 2, it could be seen that *LPD-Net V+R* performs worse than *LPD-Net R*, which shows that the place recognition cannot be improved just through virtual data augmentation. The reason for that lies in the different distribution of the point cloud caused by difference of scale across two domains, *e.g.* there is more details but more blank in the virtual point cloud frame, although they are normalized in the rectangle with the same size. *LPD-Net V* presents the worst results because of the overfitting inside the extreme regular point cloud under different environment in the virtual dataset. The performance of *vLPD-Net V* validates the generalization ability of the domain adaptation method compared to *LPD-Net V*, however, the result are limited since the quantity of virtual point cloud frames are much less than real-world frames. *vLPD-Net V+R* gives the state-of-the-art performance over all the baselines, which proves the effectiveness of domain adaptation .

Table 4. Point Cloud Registration Comparison Results on the Virtual Dataset

Model	MSE(R)	RMSE(R)	MAE(R)	MSE(t)	RMSE(t)	MAE(t)
ICP	8.4802	2.9121	1.8171	0.0225	0.1501	0.0964
FGR [33]	2096.6274	45.7889	19.1347	0.0240	0.1549	0.0915
DCP [38]	2.6111	1.6159	0.9600	0.0239	0.1546	0.1024
vLPD-Net w/o CAM (ours)	105.5031	10.2715	7.4814	0.0028	0.0527	0.0377
vLPD-Net w/o EPCOR (ours)	9.2840	3.0470	1.9358	0.0229	0.1512	0.0964
vLPD-Net (ours)	1.9317	1.3899	0.8451	0.0032	0.0568	0.0316

4.3. Ablation Study

For the ablation study, we conduct a series of comparison experiments to verify the significance contribution inside the vLPD-Net model, including the registration loss (9) for enforcement on local representation, the matching rate based metric learning (14), MMD loss (15) to address the gap of local feature across domains, and adversarial for the overall domain adaptation of feature representation.

From the ablation study results in Table 3, it could be seen adversarial training plays an important role for the whole model training to decrease the gap between two domains, significantly improving the performance of the recall rate. The evidence that the removal of MMD loss leads to the decrease of the average recall gives the hint that the alignment of local feature presents positive effects on the the domain adaptation. However, owing to the large quantity of input point-wise feature, the improvement tends to be slight compared to others. The improvement of registration loss is also limited because the NetVLAD* feature weakens the contribution of fine point-wise feature to representation learning through aggregation for compact global descriptor. Matching rate based triplet loss is valid for metric learning through the clear increase of recall.

4.4. Registration Results and Visualization

We conduct another series of experiments to validate the effectiveness of our registration network with compared to several existing approaches, *i.e.* ICP, FGR [33] and DCP [38](retrained on our dataset). The Mean Squared Error (MSE), the Root Mean Square Error (RMSE) and the Mean Absolute Error (MAE) of rotation drift (R) and translational drift (T) are selected to evaluate the performance of registration.

From the quantitative results in Table 4, our results outperform all the other. ICP falls into a local optimal without a good initial transformation while FGR fails due to lots of fake matching pairs. Compared to DCP, EPCOR provides an outlier removal method to handle patial-to-patial registration. CAM is proved to make two point clouds knowledgeable about each other and enhance the co-contextual information. The visualization of the point cloud registration is shown in Figure 6, where the vLPD-Net clearly help to align the point cloud and its retrieved one.

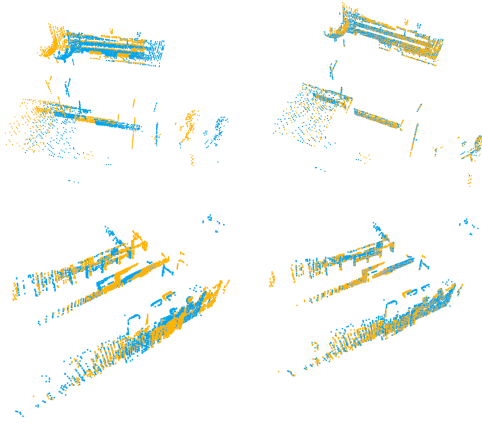


Figure 6. The visualization of point cloud registration on the right column from the initial pose on the left column through the registration network in the vLPD-Net model.

To explore the influence of structure-aware registration network on feature extraction layer, we visualize the point-wise feature from feature extraction layer by using t-SNE. We compare the dimensionality reduction feature with and without registration network from vLPD-Net in Figure 5. It could be seen that the well-retrieved paired point cloud frames through registration network retain the geometry property in the feature space while the one without registration does not, which validate the structural information can be learned by the guide of registration network.

5. Conclusion

In this work, we propose a new registration-aided domain adaptation point cloud place recognition network. A structure-aware registration network is introduced to extract the structural information of the point cloud, which has been visualized in the experiments of point cloud registration and keeps the 3D structure. Besides, the triplet loss based on matching rate is utilized for metric learning to measure the distance between point cloud frames. The impressive results of place recognition show that the adversarial training to align the point cloud representation is effective for synthetic-to-real domain adaptation.

References

[1] Deepgtav. <https://github.com/aitorzip/DeepGTAV>. 6

[2] A virtual lidar for deepgtav. <https://github.com/gdpinchina/A-virtual-LiDAR-for-DeepGTAV>. 6

[3] Mikaela Angelina Uy and Gim Hee Lee. Pointnetvlad: Deep point cloud based retrieval for large-scale place recognition. In *Proceedings of the IEEE Conference on Computer Vision and Pattern Recognition*, pages 4470–4479, 2018. 1, 2, 4, 6, 7

[4] Xuyang Bai, Zixin Luo, Lei Zhou, Hongbo Fu, Long Quan, and Chiew-Lan Tai. D3feat: Joint learning of dense detection and description of 3d local features. In *Proceedings of the IEEE/CVF Conference on Computer Vision and Pattern Recognition*, pages 6359–6367, 2020. 2

[5] Karsten M Borgwardt, Arthur Gretton, Malte J Rasch, Hans-Peter Kriegel, Bernhard Schölkopf, and Alex J Smola. Integrating structured biological data by kernel maximum mean discrepancy. *Bioinformatics*, 22(14):e49–e57, 2006. 2, 5

[6] Christopher Choy, Wei Dong, and Vladlen Koltun. Deep global registration. In *Proceedings of the IEEE/CVF Conference on Computer Vision and Pattern Recognition*, pages 2514–2523, 2020. 2, 4

[7] Nicolas Courty, Rémi Flamary, Amaury Habrard, and Alain Rakotomamonjy. Joint distribution optimal transportation for domain adaptation. In I. Guyon, U. V. Luxburg, S. Bengio, H. Wallach, R. Fergus, S. Vishwanathan, and R. Garnett, editors, *Advances in Neural Information Processing Systems*, volume 30, pages 3730–3739. Curran Associates, Inc., 2017. 2

[8] Andrea Frome, Daniel Huber, Ravi Kolluri, Thomas Bülow, and Jitendra Malik. Recognizing objects in range data using regional point descriptors. In *European conference on computer vision*, pages 224–237. Springer, 2004. 2

[9] Yaroslav Ganin and Victor Lempitsky. Unsupervised domain adaptation by backpropagation. In *International conference on machine learning*, pages 1180–1189. PMLR, 2015. 3

[10] Boqing Gong, Kristen Grauman, and Fei Sha. Connecting the dots with landmarks: Discriminatively learning domain-invariant features for unsupervised domain adaptation. In *International Conference on Machine Learning*, pages 222–230, 2013. 2

[11] Raghu Raman Gopalan, Ruonan Li, and Rama Chellappa. Domain adaptation for object recognition: An unsupervised approach. In *2011 international conference on computer vision*, pages 999–1006. IEEE, 2011. 2

[12] Kaiming He, Xiangyu Zhang, Shaoqing Ren, and Jian Sun. Deep residual learning for image recognition. In *Proceedings of the IEEE conference on computer vision and pattern recognition*, pages 770–778, 2016. 2

[13] Hanjiang Hu, Ming Cheng, Zhe Liu, and Hesheng Wang. Dasgil: Domain adaptation for semantic and geometric-aware image-based localization. *arXiv preprint arXiv:2010.00573*, 2020. 1

[14] Andrew E. Johnson and Martial Hebert. Using spin images for efficient object recognition in cluttered 3d scenes. *IEEE Transactions on pattern analysis and machine intelligence*, 21(5):433–449, 1999. 2

[15] Roman Klokov and Victor Lempitsky. Escape from cells: Deep kd-networks for the recognition of 3d point cloud models. In *Proceedings of the IEEE International Conference on Computer Vision*, pages 863–872, 2017. 2

[16] Alex Krizhevsky, Ilya Sutskever, and Geoffrey E Hinton. Imagenet classification with deep convolutional neural networks. *Communications of the ACM*, 60(6):84–90, 2017. 2

[17] Yangyan Li, Rui Bu, Mingchao Sun, Wei Wu, Xinhuan Di, and Baoquan Chen. Pointcnn: Convolution on x-transformed points. In *Advances in neural information processing systems*, pages 820–830, 2018. 2

[18] Zhe Liu, Shunbo Zhou, Chuanzhe Suo, Peng Yin, Wen Chen, Hesheng Wang, Haoang Li, and Yun-Hui Liu. Lpd-net: 3d point cloud learning for large-scale place recognition and environment analysis. In *Proceedings of the IEEE International Conference on Computer Vision*, pages 2831–2840, 2019. 1, 2, 3, 6, 7

[19] Mingsheng Long, Jianmin Wang, Guiguang Ding, Jiaguang Sun, and Philip S Yu. Transfer feature learning with joint distribution adaptation. In *Proceedings of the IEEE international conference on computer vision*, pages 2200–2207, 2013. 2, 5

[20] Yuheng Lu, Fan Yang, Fangping Chen, and Don Xie. Pic-net: Point cloud and image collaboration network for large-scale place recognition. *arXiv preprint arXiv:2008.00658*, 2020. 2

[21] Will Maddern, Geoff Pascoe, Chris Linegar, and Paul Newman. 1 Year, 1000km: The Oxford RobotCar Dataset. *The International Journal of Robotics Research (IJRR)*, 36(1):3–15, 2017. 1, 6

[22] Sinno Jialin Pan, Ivor W Tsang, James T Kwok, and Qiang Yang. Domain adaptation via transfer component analysis. *IEEE Transactions on Neural Networks*, 22(2):199–210, 2010. 2

[23] Charles R Qi, Hao Su, Kaichun Mo, and Leonidas J Guibas. Pointnet: Deep learning on point sets for 3d classification and segmentation. In *Proceedings of the IEEE conference on computer vision and pattern recognition*, pages 652–660, 2017. 2

[24] Charles Ruizhongtai Qi, Li Yi, Hao Su, and Leonidas J Guibas. Pointnet++: Deep hierarchical feature learning on point sets in a metric space. In *Advances in neural information processing systems*, pages 5099–5108, 2017. 2

[25] Can Qin, Haoxuan You, Lichen Wang, C-C Jay Kuo, and Yun Fu. Pointdan: A multi-scale 3d domain adaption network for point cloud representation. In *Advances in Neural Information Processing Systems*, pages 7192–7203, 2019. 1, 3

[26] Stephan R. Richter, Vibhav Vineet, Stefan Roth, and Vladlen Koltun. Playing for data: Ground truth from computer games. In Bastian Leibe, Jiri Matas, Nicu Sebe, and Max Welling, editors, *Computer Vision – ECCV 2016*, pages 102–118, Cham, 2016. Springer International Publishing. 6

[27] Radu Bogdan Rusu, Nico Blodow, and Michael Beetz. Fast point feature histograms (fpfh) for 3d registration. In *2009*

IEEE international conference on robotics and automation, pages 3212–3217. IEEE, 2009. 2

[28] Radu Bogdan Rusu, Nico Blodow, Zoltan Csaba Marton, and Michael Beetz. Aligning point cloud views using persistent feature histograms. In *2008 IEEE/RSJ international conference on intelligent robots and systems*, pages 3384–3391. IEEE, 2008. 2

[29] Kuniaki Saito, Kohei Watanabe, Yoshitaka Ushiku, and Tatsuya Harada. Maximum classifier discrepancy for unsupervised domain adaptation. In *Proceedings of the IEEE Conference on Computer Vision and Pattern Recognition*, pages 3723–3732, 2018. 3

[30] Samuele Salti, Federico Tombari, and Luigi Di Stefano. Shot: Unique signatures of histograms for surface and texture description. *Computer Vision and Image Understanding*, 125:251–264, 2014. 2

[31] Lukas Schaupp, Mathias Bürki, Renaud Dubé, Roland Siegwart, and Cesar Cadena. Oreos: Oriented recognition of 3d point clouds in outdoor scenarios. *arXiv preprint arXiv:1903.07918*, 2019. 2

[32] Karen Simonyan and Andrew Zisserman. Very deep convolutional networks for large-scale image recognition. *arXiv preprint arXiv:1409.1556*, 2014. 2

[33] V. A. Sindagi, Y. Zhou, and O. Tuzel. Mvx-net: Multimodal voxelnet for 3d object detection. In *2019 International Conference on Robotics and Automation (ICRA)*, pages 7276–7282, 2019. 8

[34] Richard Sinkhorn. A relationship between arbitrary positive matrices and doubly stochastic matrices. *The annals of mathematical statistics*, 35(2):876–879, 1964. 2

[35] Masashi Sugiyama, Shinichi Nakajima, Hisashi Kashima, Paul V Buenau, and Motoaki Kawanabe. Direct importance estimation with model selection and its application to covariate shift adaptation. In *Advances in neural information processing systems*, pages 1433–1440, 2008. 2

[36] Baochen Sun and Kate Saenko. Deep coral: Correlation alignment for deep domain adaptation. In *European conference on computer vision*, pages 443–450. Springer, 2016. 2

[37] Lichen Wang, Zhengming Ding, and Yun Fu. Low-rank transfer human motion segmentation. *IEEE Transactions on Image Processing*, 28(2):1023–1034, 2018. 2

[38] Yue Wang and Justin M Solomon. Deep closest point: Learning representations for point cloud registration. In *Proceedings of the IEEE International Conference on Computer Vision*, pages 3523–3532, 2019. 2, 3, 8

[39] Yue Wang and Justin M Solomon. Prnet: Self-supervised learning for partial-to-partial registration. In *Advances in Neural Information Processing Systems*, pages 8814–8826, 2019. 2, 3

[40] Yue Wang, Yongbin Sun, Ziwei Liu, Sanjay E Sarma, Michael M Bronstein, and Justin M Solomon. Dynamic graph cnn for learning on point clouds. *Acm Transactions On Graphics (tog)*, 38(5):1–12, 2019. 2

[41] Heng Yang, Jingnan Shi, and Luca Carlone. Teaser: Fast and certifiable point cloud registration. 2020. 2

[42] Jiaolong Yang, Hongdong Li, Dylan Campbell, and Yunde Jia. Go-icp: A globally optimal solution to 3d icp point-set registration. *IEEE transactions on pattern analysis and machine intelligence*, 38(11):2241–2254, 2015. 2

[43] Zi Jian Yew and Gim Hee Lee. 3dfeat-net: Weakly supervised local 3d features for point cloud registration. In *European Conference on Computer Vision*, pages 630–646. Springer, 2018. 2

[44] Zi Jian Yew and Gim Hee Lee. Rpm-net: Robust point matching using learned features. In *Proceedings of the IEEE/CVF Conference on Computer Vision and Pattern Recognition*, pages 11824–11833, 2020. 2, 4

[45] Xiangyu Yue, Bichen Wu, Sanjit A Seshia, Kurt Keutzer, and Alberto L Sangiovanni-Vincentelli. A lidar point cloud generator: from a virtual world to autonomous driving. In *Proceedings of the 2018 ACM on International Conference on Multimedia Retrieval*, pages 458–464, 2018. 1

[46] Xiangyu Yue, Bichen Wu, Sanjit A. Seshia, Kurt Keutzer, and Alberto L. Sangiovanni-Vincentelli. A lidar point cloud generator: From a virtual world to autonomous driving. In *Proceedings of the 2018 ACM on International Conference on Multimedia Retrieval*, page 458–464, New York, NY, USA, 2018. Association for Computing Machinery. 6

[47] Kun Zhang, Bernhard Schölkopf, Krikamol Muandet, and Zhiqun Wang. Domain adaptation under target and conditional shift. In *International Conference on Machine Learning*, pages 819–827, 2013. 2

[48] Wenxiao Zhang and Chunxia Xiao. Pcan: 3d attention map learning using contextual information for point cloud based retrieval. In *Proceedings of the IEEE Conference on Computer Vision and Pattern Recognition*, pages 12436–12445, 2019. 2, 6, 7

[49] Hengshuang Zhao, Li Jiang, Chi-Wing Fu, and Jiaya Jia. Pointweb: Enhancing local neighborhood features for point cloud processing. In *Proceedings of the IEEE Conference on Computer Vision and Pattern Recognition*, pages 5565–5573, 2019. 2

[50] Qian-Yi Zhou, Jaesik Park, and Vladlen Koltun. Fast global registration. In *European Conference on Computer Vision*, pages 766–782. Springer, 2016. 2

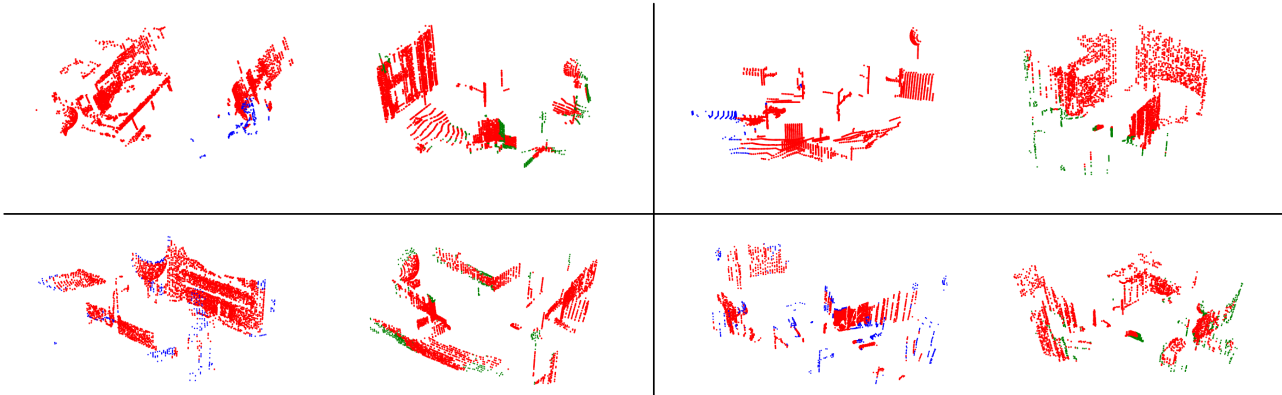


Figure 7. Visualization on negative registration. In every block, there are two point clouds: query point cloud(blue) and its negative one(green), and the red represents the outliers.

6. Supplementary Material

In this supplementary material, we provide additional details about the experiments on the virtual synthetic dataset through GTA-V, and some further visualization results.

6.1. Visualization on Positive Registration

As explained in the main paper, EPCOR is a simple but efficient iteration scheme to remove the non-matching point cloud outliers. This originates from a simple idea that an outlier tends to contribute less in the process of generating soft matching point for every point in the other point cloud. However, considering the discriminative point-wise feature has not been extracted when the network is initialized, and this method results in the absence of the gradient of some points, we remove this scheme and keep all the points as inliers at first to provide a pretrained model.

For the place recognition problem, although the retrieved pair of point clouds are in the same scene, there are still some mismatched parts. Our EPCOR indicates the distribution of these mismatched parts and helps obtain more accurate registration results. We show some visualization results of EPCOR in 8.

6.2. Visualization on Negative Registration

Generally speaking, it is meaningless to register two dissimilar point clouds. However, in the main paper, we register the query point cloud with its dissimilar point cloud to provide a matching rate based triplet loss for metric learning. This loss provides a stronger constraint on the similarity of two point clouds. For some bag-of-words approaches, the similarity depends on how many similar local features the two point clouds share. However, besides that, our proposed loss requires that matching point pair with similar local features can be aligned by rigid transformation.

It should be noted that the proposed loss relies on the pre-trained registration network. Therefore, we separately train

the registration network on virtual dataset as a pre-training model. We show some visualization results on negative registration in 7. Compared to positive registration in 8, negative registration indicates more outliers, which means the input two point clouds are dissimilar.

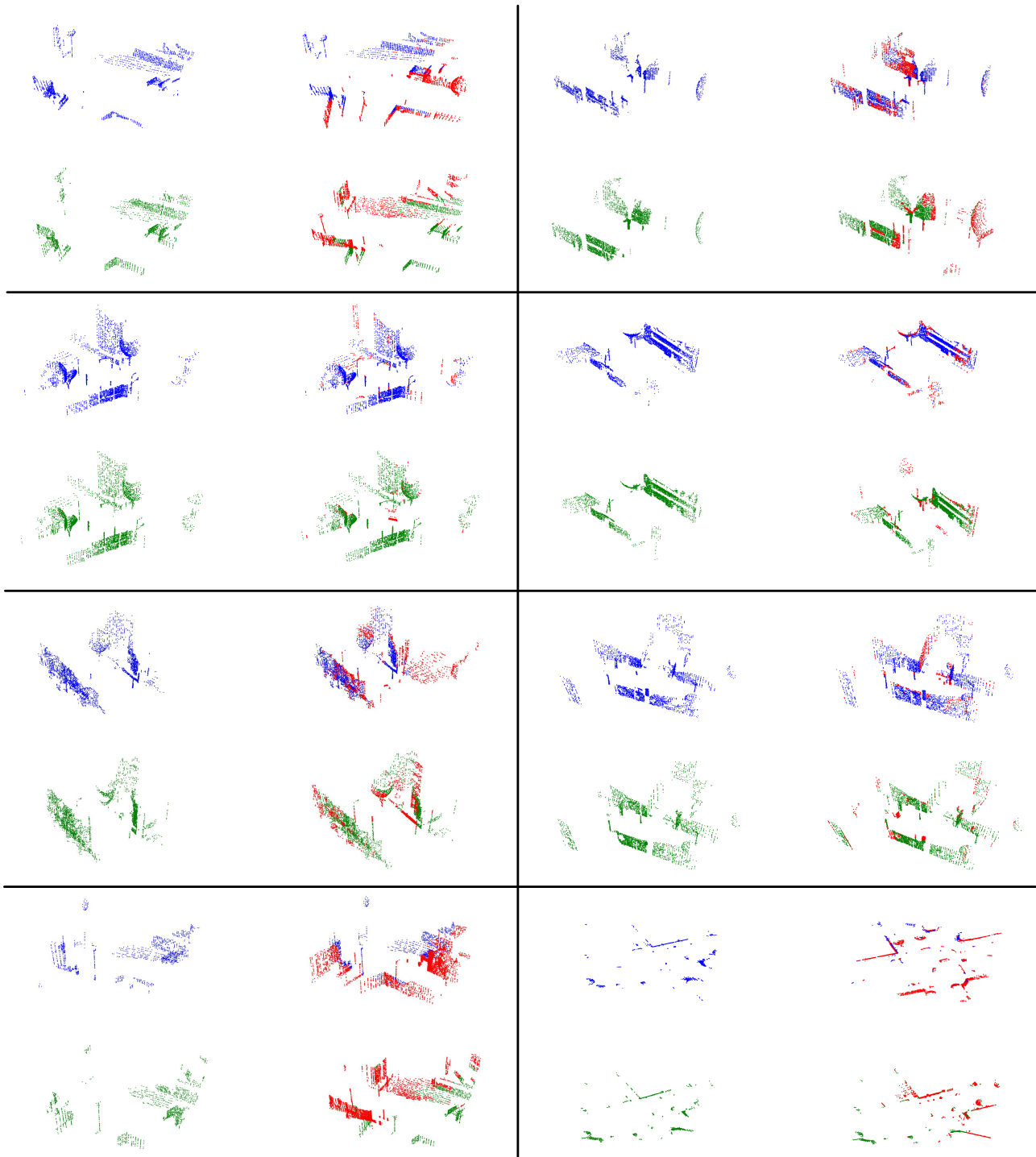


Figure 8. Visualization on EPCOR. In every block, the left side is the matching point cloud inliers of the input retrieved pair(blue and green), and the right side is the original retrieved pair and its outliers(red)